

# Observational evidence for the non-suppression effect of atmospheric chemical modification on the ice nucleation activity of East Asian dust

Jingchuan Chen<sup>1</sup>, Zhijun Wu<sup>1</sup>, Xiangxinyue Meng<sup>1</sup>, Cuiqi Zhang<sup>1</sup>, Jie Chen<sup>2</sup>, Yanting Qiu<sup>1</sup>, Li Chen<sup>1</sup>, Xin Fang<sup>1</sup>, Yuanyuan Wang<sup>3</sup>, Yinxiao Zhang<sup>3</sup>, Shiyi Chen<sup>1</sup>, Jian Gao<sup>4</sup>, Weijun Li<sup>3</sup>, and Min Hu<sup>1</sup>

<sup>1</sup>Peking University

<sup>2</sup>ETH

<sup>3</sup>Zhejiang University

<sup>4</sup>Chinese Research Academy of Environmental Sciences

November 26, 2022

## Abstract

Mineral dust alters cloud microphysical properties by acting as ice-nucleating particles (INPs). The effects of anthropogenic pollution aging on the ice nucleation activity (INA) of mineral dust are still controversial. Such effects were investigated by verifying the chemical aging of airborne size-resolved Asian dust particles via particle chemistry and morphology analyses and comparing the immersion mode INP properties of aged and normal Asian dust. The INP concentrations and ice nucleation active site densities of chemically aged supermicron dust particles (1.0-10.0  $\mu\text{m}$ ) were nearly equal to or slightly higher than those of normal Asian dust, which were 0.70-2.45 times and 0.64-4.34 times at -18  $^{\circ}\text{C}$ , respectively. These results reveal that anthropogenic pollution does not notably change the INP concentrations and does not impair the INA of Asian dust. Our work provides direct observational evidence and clarifies the non-suppression effect of anthropogenic pollution on the INA of airborne East Asian dust.

1           **Observational evidence for the non-suppression effect of atmospheric**  
2           **chemical modification on the ice nucleation activity of East Asian dust**

3 **Jingchuan Chen<sup>1</sup>, Zhijun Wu<sup>1,2\*</sup>, Xiangxinyue Meng<sup>1</sup>, Cuiqi Zhang<sup>1</sup>, Jie Chen<sup>1†</sup>, Yanting**  
4 **Qiu<sup>1</sup>, Li Chen<sup>3</sup>, Xin Fang<sup>1</sup>, Yuanyuan Wang<sup>4</sup>, Yinxiao Zhang<sup>4</sup>, Shiyi Chen<sup>1</sup>, Jian Gao<sup>5</sup>,**  
5 **Weijun Li<sup>4</sup>, and Min Hu<sup>1</sup>**

6 <sup>1</sup>State Key Joint Laboratory of Environmental Simulation and Pollution Control, College of  
7 Environmental Sciences and Engineering, Peking University, Beijing 100871, China.

8 <sup>2</sup>Collaborative Innovation Center of Atmospheric Environment and Equipment Technology,  
9 Nanjing University of Information Science and Technology, Nanjing 210044, China.

10 <sup>3</sup>Electron Microscopy Laboratory, School of Physics, Peking University, Beijing 100871, China.

11 <sup>4</sup>Department of Atmospheric Sciences, School of Earth Sciences, Zhejiang University, Hangzhou  
12 310027, China.

13 <sup>5</sup>State Key Laboratory of Environmental Criteria and Risk Assessment, Chinese Research  
14 Academy of Environmental Sciences, Beijing 100012, China.

15 <sup>†</sup>now at: Institute for Atmospheric and Climate Science, ETHZ, Zurich, 8092, Switzerland

16  
17 Corresponding author: Zhijun Wu (zhijunwu@pku.edu.cn)

18 **Key Points:**

- 19       • First direct observational evidence relating to the effects of atmospheric chemical aging  
20       on the ice nucleation of East Asian dust.
- 21       • The ice nucleation active site densities of aged supermicron particles are close to or  
22       slightly higher compared with normal Asian dust.
- 23       • Anthropogenic pollution does not impair the ice nucleation activity of East Asian dust in  
24       immersion mode.

25 **Abstract**

26 Mineral dust alters cloud microphysical properties by acting as ice-nucleating particles (INPs).  
27 The effects of anthropogenic pollution aging on the ice nucleation activity (INA) of mineral dust  
28 are still controversial. Such effects were investigated by verifying the chemical aging of airborne  
29 size-resolved Asian dust particles via particle chemistry and morphology analyses and  
30 comparing the immersion mode INP properties of aged and normal Asian dust. The INP  
31 concentrations and ice nucleation active site densities of chemically aged supermicron dust  
32 particles (1.0-10.0  $\mu\text{m}$ ) were nearly equal to or slightly higher than those of normal Asian dust,  
33 which were 0.70-2.45 times and 0.64-4.34 times at -18 °C, respectively. These results reveal that  
34 anthropogenic pollution does not notably change the INP concentrations and does not impair the  
35 INA of Asian dust. Our work provides direct observational evidence and clarifies the non-  
36 suppression effect of anthropogenic pollution on the INA of airborne East Asian dust.

## 37 Plain Language Summary

38 Airborne mineral dust triggers ice formation in clouds by acting as ice-nucleating particles  
39 (INPs), potentially influencing weather and climate at regional and global scales. Anthropogenic  
40 pollution would modify natural mineral dust during the atmospheric transport process. However,  
41 the effects of anthropogenic pollution on the ice nucleation activity of mineral dust remain not  
42 well-understood. In this study, we investigated the ice nucleation properties and particle  
43 chemical characterizations of collected size-resolved Asian dust samples, and testified the  
44 chemical modification of aged dust particles according to the mass concentrations of particulate  
45 matter, the water-soluble ion concentrations, the metal element concentrations, and single-  
46 particle morphology. The INP concentrations and nucleation activities of aged supermicron  
47 Asian dust (1.0 to 10.0  $\mu\text{m}$ ) were similar to or slightly higher than those of normal Asian dust,  
48 but the difference was not statistically significant. Therefore, anthropogenic pollution does not  
49 notably change the INP concentrations and does not impair the ice nucleation activity of Asian  
50 dust. This study provides direct observation of naturally aged mineral dust to evaluate the  
51 comprehensive effect of anthropogenic pollution on the ice nucleation activity of Asian dust,  
52 advancing the understanding of the ice nucleation of airborne aged mineral dust.

## 53 1 Introduction

54 Heterogeneous ice nucleation is a key process in mixed-phase clouds, influencing the water  
55 partitioning between ice and liquid phase, and further determining the lifetime, radiative forcing,  
56 and precipitation of clouds (Lohmann et al., 2016; Murray et al., 2012). Mineral dust is one of  
57 the most important sources of ice-nucleating particles (INPs) due to its high atmospheric loading  
58 (Textor et al., 2006), efficient ice nucleation activity (INA) (Hoose & Mohler, 2012), and long-  
59 range and even global transport capacity (Pratt et al., 2009; Uno et al., 2009). During the long-  
60 range transport, dust particles may mix, adsorb, coagulate or react with other substances (such as  
61 biological materials, anthropogenic emissions, and secondary products), and these coatings or  
62 reactants may in turn alter the INA of mineral dust (Kanji et al., 2017), affecting cloud formation  
63 and their microphysical properties.

64 Satellite observations and model simulations reported that a considerable fraction of  
65 anthropogenic pollutants can act as INPs to catalyze ice formation in clouds (B. Zhao et al.,  
66 2019). However, recent studies have found that anthropogenic pollution, particularly black  
67 carbon (BC), does not significantly influence regional, global and historical INP concentrations  
68 ( $N_{INP}$ ) relevant to mixed-phase clouds (J. Chen et al., 2018b; Hartmann et al., 2019; Schill et al.,  
69 2020). These studies answer the question of anthropogenic contributions to  $N_{INP}$  to some extent,  
70 but the understanding of effects of anthropogenic activities on the INA of natural INPs such as  
71 mineral dust remains to be clarified.

72 Previous laboratory studies have evaluated the effects of various reactants/coatings on the  
73 freezing activities of dust INPs. Although the same substance would have different aging effects  
74 among different studies due to their experimental design, reaction conditions, and mineral types,  
75 most immersion freezing studies agreed that not all inorganic acids reduced the INA of dust  
76 particles as H<sub>2</sub>SO<sub>4</sub> did (Cziczo et al., 2009; Niedermeier et al., 2010; Sullivan et al., 2010b); the  
77 exposure to HNO<sub>3</sub> suggested no distinct impact (Kulkarni et al., 2015; Sullivan et al., 2010a);  
78 organic coatings (e.g., levoglucosan) also had an unobservable impact (Kanji et al., 2019; Tobo et  
79 al., 2012; Wex et al., 2014); and NH<sub>4</sub><sup>+</sup> and K<sup>+</sup> enhanced the INA of dust (Whale et al., 2018;  
80 Worthy et al., 2021; Yun et al., 2020). These deactivation, equivalence, or enhancement effects  
81 of varying substances on mineral dust would coexist in the real atmosphere and finally result in a  
82 combined effect. Therefore, the actual effect of atmospheric aging on mineral dust, a  
83 comprehensive result of multi-species and complex mechanisms, may differ from laboratory  
84 aging experiments based on a single substance. In model simulations, the coating effect may  
85 obviously alter the INA of particles according to different assumptions (Kulkarni et al., 2015; J.  
86 L. Zhu & Penner, 2020), further influencing ice formation in clouds and consequent climate  
87 effect. However, the field observation relating to the ice nucleation of mineral dust aged in a real  
88 atmosphere is very scarce, which limits the verification of laboratory results and the updating of  
89 parameterized schemes in model simulations.

90 Asian dust is the second largest source of dust INPs in the world, and can more efficiently trigger  
91 ice nucleation in mixed-phase clouds (Froyd et al., 2022; Kawai et al., 2021). In the downwind  
92 of East Asian dust transport path, the severe anthropogenic air pollution occasionally occurred in  
93 North China could chemically and/or physically modify these dust particles (Huang et al., 2010;  
94 Wu et al., 2020), thus changing the ice nucleation properties of Asian dust. In this study, airborne  
95 mineral dust samples were collected during Asian dust events and aged dust periods, respectively.  
96 The chemical modification of aged Asian dust particles was confirmed by multiple lines of  
97 experimental evidence. On this basis, we compared the INP concentrations and activities of aged  
98 and normal Asian dust from the overall and size-resolved perspectives. This study provides  
99 direct observation evidence to evaluate the comprehensive effect of anthropogenic pollution on  
100 the INA of Asian dust, advancing the understanding of the ice nucleation of airborne aged  
101 mineral dust.

## 102 2 Materials and Methods

### 103 2.1 Sample collection

104 The samples were collected at the Peking University Atmosphere Environment Monitoring  
 105 Station (39.99 N, 116.31 E) during the Asian dust events in the spring of 2018 and 2019. An  
 106 eight-stage Micro-Orifice Deposit Impactor (MOUDI, model 100-R, MSP Corporation, USA)  
 107 with aerodynamic cut-off diameter ( $D_{50}$ ) ranging from 0.18 to 10  $\mu\text{m}$  at a flow rate of 30  $\text{L min}^{-1}$   
 108 (Marple et al., 1991) was applied with polycarbonate filters (47 mm Nuclepore, 0.2  $\mu\text{m}$  pores,  
 109 Whatman) to collect size-resolved aerosol samples during the Asian dust events, which were  
 110 forecasted and monitored by China Meteorological Administration (Text S1).

### 111 2.2 INP measurements and calculations

112 As described in J. C. Chen et al. (2021), the sampled filter of each MOUDI stage was extracted  
 113 by an ultrasonic shaker in 20 mL double-distilled water (resistivity of 18.2  $\text{M}\Omega\text{ cm}$  at 25  $^{\circ}\text{C}$ ) for  
 114 30 min to shake the particles off the filter. Thus, suspended samples containing mineral dust  
 115 particles were obtained for further INP measurements and chemical analyses.

116 The PeKing University Ice Nucleation Array (PKUINA), a cold-stage-based instrument, was  
 117 employed to perform immersion freezing measurements (J. Chen et al., 2018a). Briefly, 90  
 118 droplets (1  $\mu\text{L}$ ) of suspensions were pipetted onto a hydrophobic glass slide located on the cold  
 119 stage in each experiment. These droplets were separated from each other by a spacer block and  
 120 upper and lower glass slides to prevent the Wegener-Bergeron-Findeisen process. A charge-  
 121 coupled device was employed to monitor the cooling process (cooling rate 1  $^{\circ}\text{C min}^{-1}$ ) of the  
 122 cold stage (one frame every 6 s) until all 90 droplets were frozen.

123 The cumulative number concentration of INP ( $N_{INP}$ ) per unit volume of sampled air (Vali, 1971)  
 124 is calculated as:

$$N_{INP}(T) = \frac{-\ln(1 - f_{ice}(T))}{V_{air}} (\text{L}^{-1} \text{ air}) \quad (1)$$

125 where  $f_{ice}(T)$  is the fraction of frozen droplets in the total 90 droplets above temperature  $T$ , and  
 126  $V_{air}$  is the total volume of sampled air per droplet (standard conditions, 0  $^{\circ}\text{C}$ , 1013 hPa) during  
 127 each sampling period.

128 As a comparable parameter of INA commonly used for mineral dust, the cumulative ice  
 129 nucleation active site density  $n_s$  (Connolly et al., 2009; Niemand et al., 2012), i.e., the number of  
 130 active sites per unit surface area of INPs (Vali et al., 2015) is derived from the  $N_{INP}$  as:

$$n_s(T) = \frac{N_{INP}(T)}{A} \text{ (m}^{-2}\text{)} \quad (2)$$

131 where  $A$  is the total surface area of particles derived from the online particle number-size  
 132 distribution measurements within a unit volume of sampled air (aerodynamic diameter, spherical  
 133 particle hypothesis, 0 °C, 1013 hPa).

134 Note that, in this study,  $N_{INP}(T)$  and  $n_s(T)$  for each particle size class (referred to as  $N_{INP}(T)$   
 135 and  $n_s(T)$ ) and all particle size spectrum (0.18-10  $\mu\text{m}$ , referred to as total  $N_{INP}(T)$  and total  
 136  $n_s(T)$ ) were calculated. The total  $N_{INP}(T)$  is a sum of size-resolved  $N_{INP}(T)$  ranging from 0.18  
 137 to 10  $\mu\text{m}$  during each dust event. Whereas, the total  $n_s(T)$  is the value of total  $N_{INP}(T)$  divided  
 138 by the total surface area of particles in all size classes.

### 139 2.3 Particulate matter measurements and chemical analysis

140 The mass concentrations of particulate matter  $\leq 2.5 \mu\text{m}$  ( $\text{PM}_{2.5}$ ) and 10  $\mu\text{m}$  ( $\text{PM}_{10}$ ), the BC mass  
 141 concentration, and the number-size distributions of particulate matter were measured throughout  
 142 the sampling periods by TH2000Z1 (Text S2), Multi-Angle Absorption Photometer (MAAP,  
 143 Text S3), and Scanning Mobility Particle Sizers (SMPS, Text S4) coupled with Aerodynamic  
 144 Particle Sizer (APS, Text S4), respectively. The time resolution for TH2000Z1 was 1 min, and  
 145 for MAAP, SMPS, and APS was 5 min.

146 Water-soluble ions and elemental composition in the extracted Asian dust samples (suspensions)  
 147 were analyzed. For water-soluble inorganic ions ( $\text{Na}^+$ ,  $\text{Mg}^{2+}$ ,  $\text{K}^+$ ,  $\text{Ca}^{2+}$ ,  $\text{NH}_4^+$ ,  $\text{NO}_3^-$ ,  $\text{SO}_4^{2-}$ , and  
 148  $\text{Cl}^-$ ), the suspension was firstly filtered by Polyethersulfone (PES) membrane filters (0.45  $\mu\text{m}$ ),  
 149 and then it was detected by Ion Chromatography (IC, DIONEX ICS-2000/Integrion, Text S5).  
 150 As for elemental composition (Al, K, Mn, Mg, Ca, Cu, Pb, and Zn), the suspensions containing  
 151 particles underwent pretreatments until all particles were digested, and then they were  
 152 determined by the Inductively Coupled Plasma Mass Spectrometry (ICP-MS, XSeries 2, Text  
 153 S6).

## 154 3 Results and Discussion

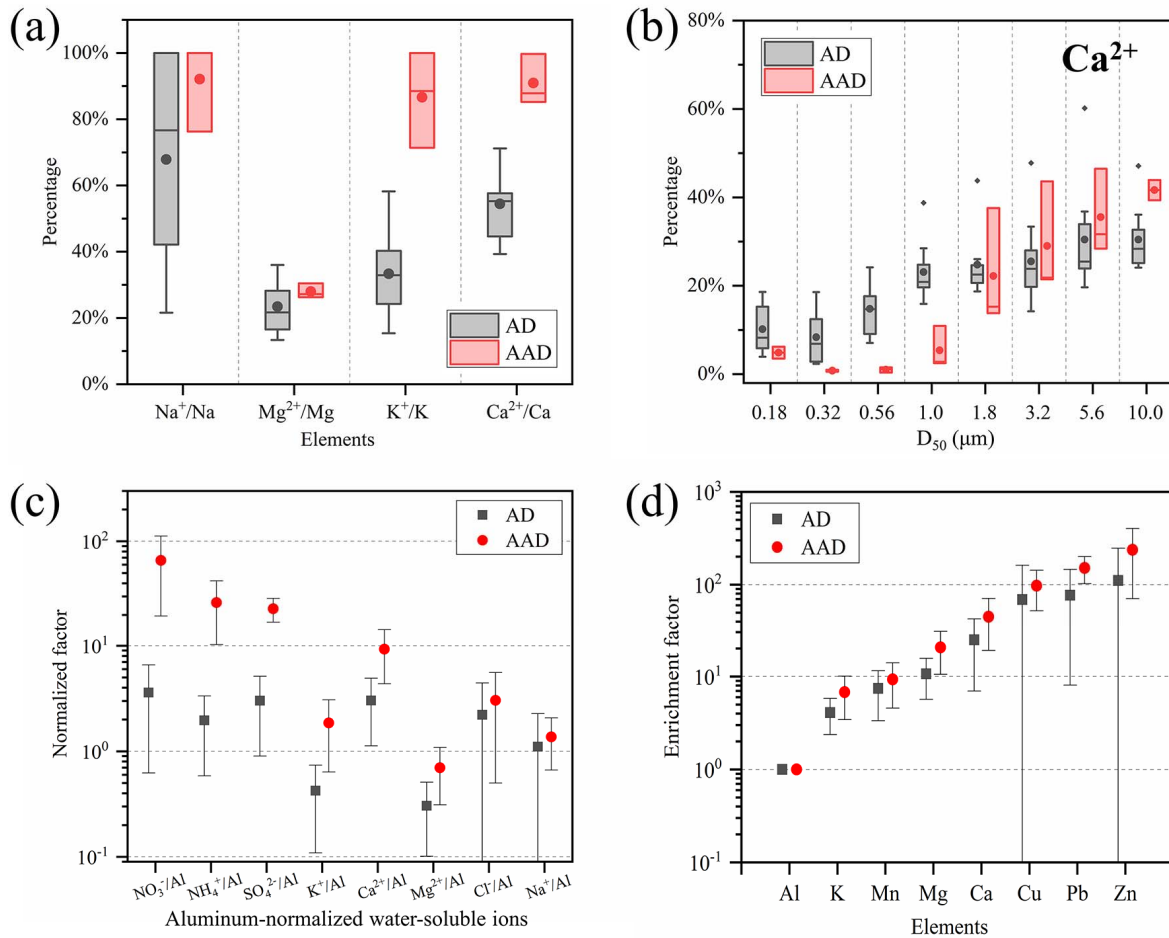
### 155 3.1 Observational evidence of chemically modified Asian dust particles

156 The collected samples were categorized as aged Asian dust (AAD hereafter, three samples  
 157 including M8, D2, and D5) and Asian dust (AD hereafter, nine samples including M2, M3, M5,  
 158 M6, M7, D3, D4, D6, and D7) based on the particle number-size distributions and mass

159 concentrations, gaseous pollutants, and meteorological parameters during the sampling periods  
160 (Figure S1, S2, Table S1, and Text S7). On average, PM<sub>10</sub> concentrations of the AD and AAD  
161 samples were  $227.2 \pm 123.9$  and  $203.9 \pm 47.5 \mu\text{g m}^{-3}$ , respectively, suggesting similar  
162 atmospheric dust mass loading. Whereas, the concentrations of PM<sub>2.5</sub> and BC in AAD were more  
163 than twice as high as those in AD ( $103.7 \pm 25.4$  vs  $43.3 \pm 17.7 \mu\text{g m}^{-3}$  for PM<sub>2.5</sub> and  $2.90 \pm 0.37$   
164 vs  $1.33 \pm 0.64 \mu\text{g m}^{-3}$  for BC). And the ratio of PM<sub>2.5</sub> to PM<sub>10</sub> in AAD was 50.8%, which was  
165 much higher than that in AD (19.1%), indicating that there were much more anthropogenic  
166 pollutants mixed with dust particles during the AAD periods.

167 Previous studies have already shown that chemical aging processes enhanced the water-soluble  
168 ions by heterogeneous reactions and/or coagulation of CaCO<sub>3</sub> with acidic gases (e.g. NO<sub>2</sub>, HNO<sub>3</sub>,  
169 SO<sub>2</sub>, and H<sub>2</sub>SO<sub>4</sub>) and secondary aerosols (e.g. NH<sub>4</sub>NO<sub>3</sub> and (NH<sub>4</sub>)<sub>2</sub>SO<sub>4</sub>) (Fairlie et al., 2010;  
170 Laskin et al., 2005; Underwood et al., 2001; T. Zhu et al., 2011). The mineral composition  
171 CaCO<sub>3</sub> (~5-30%) was converted to more water-soluble Ca(NO<sub>3</sub>)<sub>2</sub> or CaSO<sub>4</sub> during transport  
172 (McNaughton et al., 2009). In the aqueous layer facilitated by Ca(NO<sub>3</sub>)<sub>2</sub>, CaSO<sub>4</sub> and NH<sub>4</sub><sup>+</sup> can  
173 rapidly form by the coagulation of particulate (NH<sub>4</sub>)<sub>2</sub>SO<sub>4</sub> with dust (Heim et al., 2020).  
174 Moreover, NH<sub>4</sub>NO<sub>3</sub> can efficiently form on the surface of saline mineral particles (Wu et al.,  
175 2020). Therefore, we propose to use the fraction of water-soluble ion in corresponding elemental  
176 concentration ( $f_{wsice}$ ), that is, the ratio of water-soluble ion concentration to corresponding  
177 element concentration in the sample, to evaluate the degree of chemical modification of dust  
178 particles.

179 As illustrated in Figure 1 (a) and Table S2, the mean  $f_{wsice}$  values of four mental elements (Na,  
180 Mg, K, and Ca) were much higher in AAD, especially for Ca, which increased by 67.0% to  $90.9$   
181  $\pm 6.3\%$  compared with AD ( $54.4 \pm 10.3\%$ ). Moreover, size-resolved water-soluble ion analysis  
182 revealed that the mean relative mass proportions of Ca<sup>2+</sup> in supermicron AAD particles ( $1.0 \mu\text{m}$   
183  $< D_p \leq 10 \mu\text{m}$ ) were higher (3.5-11.2%) than those in AD (Figure 1 (b) and Table S3). Combined  
184 with the higher relative mass proportions of NO<sub>3</sub><sup>-</sup> (4.8-18.5%, Figure S3 and Table S3), the  
185 significant increase of Ca<sup>2+</sup> in supermicron particles demonstrated the formation of  
186 heterogeneous reaction product Ca(NO<sub>3</sub>)<sub>2</sub> and the more pronounced chemical aging of AAD.



187

188 **Figure 1.** Chemical modification analyses of AD and AAD samples. (a) Fractions of water-  
 189 soluble ion in corresponding elemental concentration ( $f_{wsice}$ ) were derived from their IC and  
 190 ICP-MS measurements. (b) Relative mass proportions of water-soluble calcium ions ( $\text{Ca}^{2+}$ ) in  
 191 size-resolved AD and AAD samples. (c) Aluminum-normalized water-soluble ions (AWSIs)  
 192 were the ratio of the concentrations of water-soluble ions to the concentration of reference  
 193 element Al in the samples. (d) Enrichment factors were derived from the elemental  
 194 concentrations of aerosol and crust with the reference element Al. Nine AD samples and three  
 195 AAD samples were analyzed, and they are colored by gray and red, respectively. In the box plot  
 196 (a) and (b), The boxes represent the interquartile range (IQR,  $\text{IQR} = \text{Q3} - \text{Q1}$ ). The whiskers  
 197 represent the range within  $1.5 * \text{IQR}$ . The solid lines, solid circles, and solid diamonds represent  
 198 the median, mean, and outlier, respectively. Values greater than  $\text{Q3} + (1.5 * \text{IQR})$  or less than  $\text{Q1}$   
 199  $- (1.5 * \text{IQR})$  are defined as outliers. In the scatter plot (c) and (d), AD and AAD are presented as  
 200 solid gray squares and solid red circles, respectively. Error bars are the standard deviations.  
 201

202 We also calculated the aluminum-normalized water-soluble ions (AWSIs) to quantify the degree  
 203 of particle aging. Aluminum is a major crustal conservative element with constancy and is often  
 204 used as a reference element for dust particles (Lawson & Winchester, 1979). Thus, the three

205 anions and five cations were divided by the concentration of Al respectively to obtain the  
206 normalized parameters in Figure 1 (c). Compared with AD, the AWSIs of AAD samples were  
207 about one order of magnitude (7.6-18.3 times) higher for aluminum-normalized  $\text{NO}_3^-$ ,  $\text{NH}_4^+$ , and  
208  $\text{SO}_4^{2-}$  (sulfate, nitrate, and ammonium ions, SNA); 2.3-4.4 times higher for  $\text{K}^+$ ,  $\text{Ca}^{2+}$ , and  $\text{Mg}^{2+}$ ;  
209 and similar (1.2-1.4 times) for  $\text{Cl}^-$  and  $\text{Na}^+$  (Table S4 and S5). The aging products represented by  
210 aluminum-normalized SNA and  $\text{Ca}^{2+}$  were much higher in AAD, which once again proved that  
211 AAD samples had undergone more remarkable atmospheric chemical aging.

212 Enrichment factors (EFs) of eight elements in AD and AAD are illustrated in Figure 1 (d). The  
213 EFs were calculated by the normalization of elemental concentrations in aerosol and crust  
214 respected to those of a reference element (Barbieri, 2016). In this study, Al was the reference  
215 element and the crustal abundance was given by Wei et al. (1991), so that EF was calculated as  
216  $\text{EF} = (\text{X}/\text{Al})_{\text{aerosol}} / (\text{X}/\text{Al})_{\text{crust}}$ . Average EFs in AD and AAD samples were generally ranging  
217 from 1 to 10 for Al, K, and Mn, suggesting the crustal origin; ranging from 10 to 100 for Mg, Ca,  
218 and Cu, suggesting both crustal and anthropogenic origin; >100 for Pb and Zn, implying a  
219 significant enrichment from anthropogenic origin. The element EFs of AAD were all about twice  
220 as much as those of AD, indicating that the dust particles were more affected by anthropogenic  
221 activities during the AAD periods.

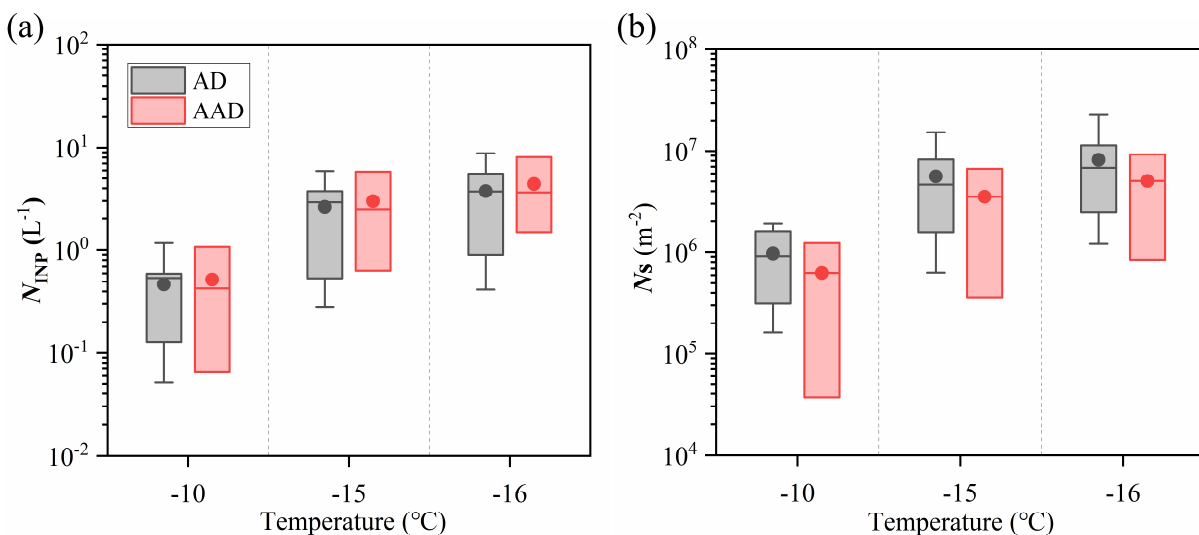
222 Environmental scanning electron microscopy (ESEM) and transmission electron microscopy  
223 (TEM) analyses (Kiselev et al., 2017; Li et al., 2016) provided detailed information on collected  
224 particles (Figure S4, S5, S6, and Text S8), and the particle morphology of modified Asian dust  
225 was observed. In an AAD sample, both mineral dust (Figure S7) and anthropogenic pollutants  
226 (soot, i.e., BC, Figure S8) were present, and minerals, soot, organics, and inorganics were  
227 internally mixed (Figure S9 and S10), meaning that dust particles were aged by physical  
228 adsorption and/or chemical reactions during the AAD periods. Similar results were also reported  
229 in previous studies. Li and Shao (2009) found that visible coatings (mainly nitrates) were on the  
230 surface of most mineral particles (~90%) during brown haze in Beijing, and up to 32% of dust  
231 particles were coated with  $\text{Ca}(\text{NO}_3)_2$  in Asian outflow (Li et al., 2014).

232 In conclusion, we demonstrated that the AAD samples have been significantly aged in the  
233 anthropogenic polluted atmosphere. By contrast, the chemical aging degree of AD was notably  
234 lower than that of AAD. Based on the aging differences between AD and AAD, the influence of

235 anthropogenic pollution on the ice nucleation properties of Asian dust would be investigated in  
 236 the following sections.

### 237 3.2 Effects of anthropogenic pollution on the ice nucleation of Asian dust

238 Figure 2 (a) presents the total  $N_{INP}$  of AD and AAD samples, which were  $0.47 \pm 0.34$  and  $0.52 \pm$   
 239  $0.42 \text{ L}^{-1}$  at  $-10 \text{ }^\circ\text{C}$ ,  $2.63 \pm 2.04$  and  $2.99 \pm 2.15 \text{ L}^{-1}$  at  $-15 \text{ }^\circ\text{C}$ , and  $3.75 \pm 2.90$  and  $4.41 \pm 2.75 \text{ L}^{-1}$   
 240 at  $-16 \text{ }^\circ\text{C}$  (Table S6), respectively. Although the AAD particles were modified by anthropogenic  
 241 pollutants, they were in the same INP concentration range (1.11-1.18 times for mean total  $N_{INP}$ )  
 242 as AD samples at  $-10$ ,  $-15$ , and  $-16 \text{ }^\circ\text{C}$ . There was no statistically significant difference between  
 243 the total  $N_{INP}$  of AD and AAD (Two-Sample Independent t-Test,  $p > 0.05$ , Text S9),  
 244 demonstrating that anthropogenic pollution did not increase or decrease the  $N_{INP}$  of natural dust  
 245 particles. This conclusion is consistent with previous studies showing that anthropogenic  
 246 pollution has not affected  $N_{INP}$  (J. Chen et al., 2018b; Hartmann et al., 2019).



247

248 **Figure 2.** Effects of anthropogenic pollution on the INP concentrations and activities of AD and  
 249 AAD samples. (a) Total INP concentrations (total  $N_{INP}$ ) and (b) total ice nucleation active site  
 250 density (total  $n_s(T)$ ) of AD and AAD samples at three temperatures are colored by gray and red,  
 251 respectively. Nine AD samples and three AAD samples were involved in the analysis and  
 252 displayed in box plot. The boxes represent the interquartile range (IQR,  $\text{IQR} = \text{Q3} - \text{Q1}$ ). The  
 253 whiskers represent the range within  $1.5 \times \text{IQR}$ . The solid lines and solid circles represent the  
 254 median and mean, respectively.  
 255

256 As depicted in Figure 2 (b), the mean total  $n_s(T)$  of AAD samples at three temperatures were  
 257 slightly lower (0.62-0.65 times) than those of AD samples (Table S6), while the lower quartile

258 (such as at -10 °C) was up to an order of magnitude lower. Compared with AD, there were more  
259 non-dust particles (e.g. urban pollution aerosols) in the submicron AAD ( $D_p < 1.0 \mu\text{m}$ ). These  
260 submicron anthropogenic particles contributed less to total  $N_{INP}$  than high-activity dust, but had  
261 a much higher particle surface area (Figure S11), resulting in a lower total  $n_s(T)$  for AAD.  
262 Therefore, the actual effects of anthropogenic pollution on the INA of Asian dust need to be  
263 further investigated from a size-resolved perspective.

### 264 3.3 Aging effects on the ice nucleation of size-resolved Asian dust

265 The effects of anthropogenic pollution on the INP concentrations and activities of size-resolved  
266 particles at -15 and -18 °C are depicted in Figure 3 (a)-(d). Compared with AD, the  $N_{INP}$  of AAD  
267 were an order of magnitude lower for  $D_{50} = 0.18$  and  $0.32 \mu\text{m}$ ; consistent for  $D_{50} \geq 0.56 \mu\text{m}$   
268 (such as 0.70-2.45 times at -18 °C, Table S7). Similarly, for particles with  $D_{50} < 1.0 \mu\text{m}$ , the  
269  $n_s(T)$  of AAD samples were 1 to 2 orders of magnitude lower than those of AD, while aged dust  
270 was nearly equal to or even more active than AD for  $D_{50} \geq 1.0 \mu\text{m}$  at given temperatures (e.g.  
271 0.64-4.34 times at -18 °C). There was a more pronounced size-dependent freezing ability in  
272 AAD samples, spanning 5 orders of magnitude, implying that different types of INPs may be  
273 included. Combined with the much lower  $N_{INP}$  of submicron AAD, we think these much less  
274 active submicron INPs were more likely to be anthropogenic pollutant particles in urban areas.  
275 That is, AAD samples were mainly composed of submicron urban pollution particles and  
276 significantly aged supermicron Asian dust.

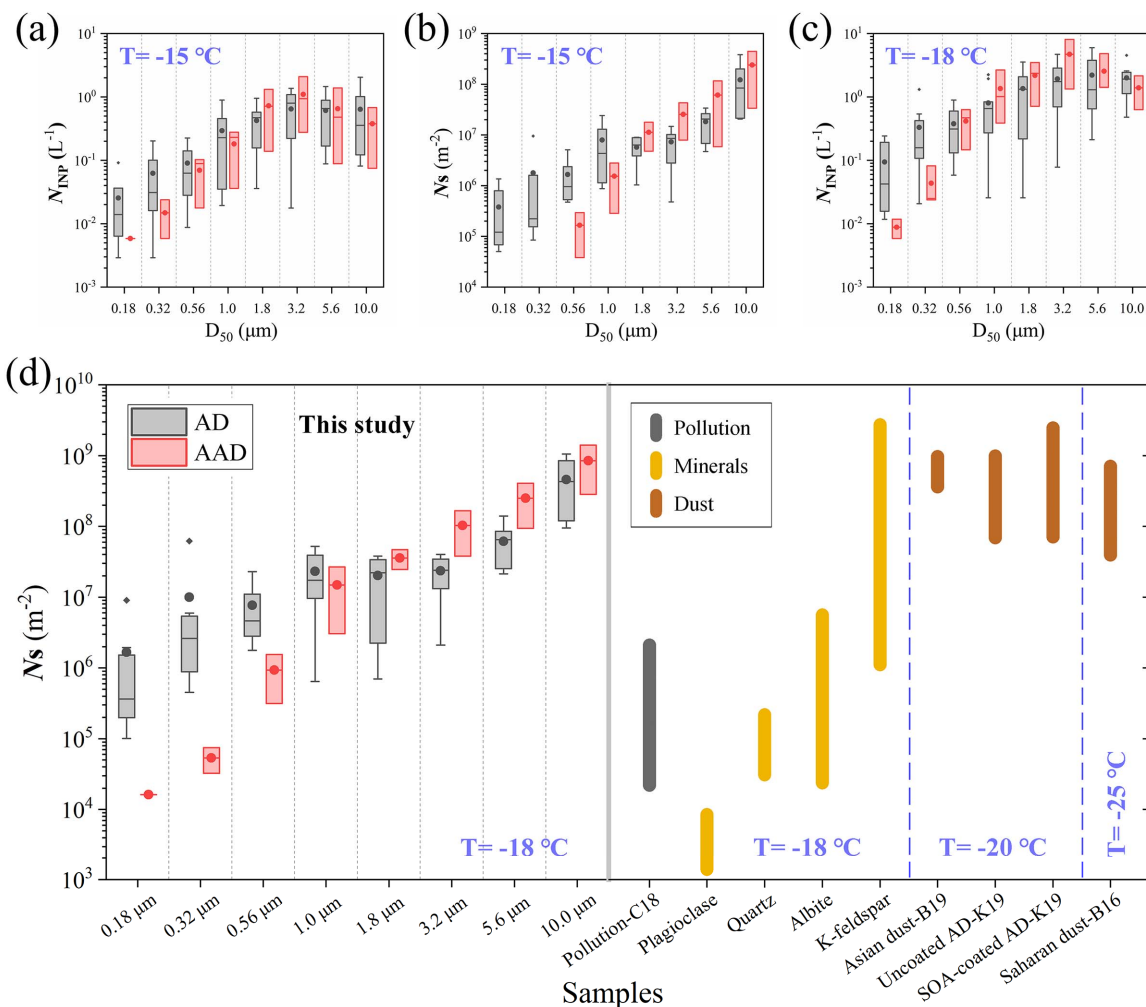
277 To testify above point, we also compared the  $n_s(T)$  in this study with urban pollution particles  
278 (Pollution-C18 (J. Chen et al., 2018b), marked by dark gray), reference minerals (plagioclase,  
279 quartz, albite, and K-feldspar (Harrison et al., 2019), marked by yellow), and dust particles  
280 (Asian dust-B19 (Bi et al., 2019), Uncoated AD-K19 (Kanji et al., 2019), and Saharan dust-B16  
281 (Boose et al., 2016), marked by brown) in Figure 3 (d). The  $n_s(T)$  of submicron AAD ( $D_{50} =$   
282  $0.18, 0.32, \text{ and } 0.56 \mu\text{m}$ ) were in the same range as Pollution-C18. On the other hand,  
283 considering the lower measurement temperatures (-20/-25 °C) in literature studies, the  
284 supermicron particles for both AD and AAD samples in this study presented comparable INA  
285 with Asian dust-B19 ( $D_{50} = 2.5 \mu\text{m}$ ), Uncoated AD-K19 ( $0.01\text{-}3 \mu\text{m}$ ), Saharan dust-B16  
286 ( $D_{50} = 3.5 \mu\text{m}$ ), and K-feldspar, which were more active than many minerals such as albite,

287 plagioclase, and quartz, demonstrating that these supermicron particles in AD and AAD were  
 288 authentic mineral dust.

289 For supermicron dust particles, the AAD presented similar or slightly higher nucleation activity  
 290 than AD, but the difference was not statistically significant ( $p > 0.05$ ). In other words, the INA of  
 291 Asian dust did not decrease after atmospheric aging. This conclusion was supported by Kanji et  
 292 al. (2019), who found that there was no systematic difference between SOA-coated and uncoated  
 293 Asian dust (Uncoated AD-K19 and SOA-coated AD-K19 in Figure 3 (d), Table S8, and S9).

294 Similarly, Boose et al. (2016) reported a small positive effect of anthropogenic emissions on the  
 295 Sahara dust. Based on lidar measurements, He et al. (2021) also revealed that, after long-range  
 296 transport, the INA of Asian dust mixed with pollutants did not distinctly change. Therefore, we  
 297 conclude that anthropogenic pollution does not impair the INA of airborne Asian dust.

298



299

300 **Figure 3.** Comparison of the INP concentrations ( $N_{INP}$ ) and ice nucleation active site densities  
 301 ( $n_s(T)$ ) among AD, AAD, and literature samples. (a)  $N_{INP}$  at -15 °C. (b)  $n_s(T)$  at -15 °C. (c)  
 302  $N_{INP}$  at -18 °C. (d)  $n_s(T)$  at -18, -20, and -25 °C. Size-resolved AD and AAD samples in this  
 303 study are colored by gray and red, respectively, and grouped by particle size classes. The boxes  
 304 represent the interquartile range (IQR,  $IQR = Q3 - Q1$ ). The whiskers represent the range within  
 305  $1.5 * IQR$ . The solid lines, solid circles, and solid diamonds represent the median, mean, and  
 306 outlier, respectively. Values greater than  $Q3 + (1.5 * IQR)$  or less than  $Q1 - (1.5 * IQR)$  are  
 307 defined as outliers. The  $n_s(T)$  of urban pollution particles (Pollution-C18 (J. Chen et al., 2018b),  
 308 marked by dark gray), reference minerals (Plagioclase, Quartz, Albite, and K-feldspar (Harrison  
 309 et al., 2019), marked by yellow), and dust particles (Asian dust-B19 (Bi et al., 2019), Uncoated  
 310 AD-K19 (Kanji et al., 2019), SOA-coated AD-K19 (Kanji et al., 2019), and Saharan dust-B16  
 311 (Boose et al., 2016), marked by brown) at -18 °C (or -20/-25 °C) are shown for comparison. Note  
 312 that the four types of mineral dust particles were summarized by Harrison et al. (2019), and the  
 313 data were measured in previous studies (Atkinson et al., 2013; Augustin-Bauditz et al., 2014;  
 314 DeMott et al., 2018; Harrison et al., 2019; Harrison et al., 2016; Losey et al., 2018; Niedermeier  
 315 et al., 2015; O'Sullivan et al., 2014; Peckhaus et al., 2016; Reicher et al., 2018; Whale et al.,  
 316 2015; Zolles et al., 2015).

317

318 Previous studies have proposed a variety of possible explanations for aging effects based on  
 319 single substance (e.g.  $HNO_3$  or  $(NH_4)_2SO_4$ ) aging experiments. One special aspect of this study  
 320 is that the dust aging process took place in the atmosphere, thus the observed non-suppression  
 321 effect of INA by atmospheric aging was a comprehensive reflection of multiple possible  
 322 reactants and influencing mechanisms. First, alkaline calcite and carbonate might not be good  
 323 INPs. They could react with acids such as  $HNO_3$  and would move away from the surface of  
 324 particles in the immersion freezing mode due to the dissolution of water-soluble reaction  
 325 products in a liquid environment. But new surface-active sites of unreacted particles could be  
 326 exposed in this process. Second, water-soluble coatings (e.g.  $NO_3^-$  and  $SO_4^{2-}$ ) may not affect the  
 327 INA of Asian dust. These substances are dissolved and reversibly desorbed from particle  
 328 surfaces during hygroscopic growth and droplet activation, revealing the concealed active sites  
 329 and unaffacting freezing (Sullivan et al., 2010a). Third, ion exchange including the suppression  
 330 of  $H^+$  (Augustin-Bauditz et al., 2014; Kumar et al., 2018; Wex et al., 2014) and the enhancement  
 331 of  $NH_4^+/K^+$  (Whale et al., 2018; Yun et al., 2020) is likely related to the change of mineral INA.  
 332 According to the pH-dependent suppression theory from Yun et al. (2021), there is no obvious  
 333 suppression effect at  $pH > 5$ . Mineral dust particles are alkaline and can maintain high pH ( $pH =$   
 334  $5-7$ ) in the atmosphere (Pye et al., 2020), especially for the supermicron dust particles (Fang et  
 335 al., 2017). During the severe air pollution periods in China, the particle pH was also about 4-5  
 336 and increased in recent years (Song et al., 2019; Xie et al., 2020). Therefore, the suppression

337 effect of  $H^+$  on the INA of dust is very limited at the near-neutral particle reaction interface. On  
338 the contrary, there is a large amount of  $NH_4^+$  in the ammonia-rich atmosphere of China (Meng et  
339 al., 2020; M. Zhao et al., 2016), which may form more active surfaces and enhance the  
340 nucleation activity of Asian dust. Finally, the hydrogen bond derived from oxidized hydroxyl  
341 groups and adsorbed  $NH_4^+$  could promote ice nucleation on the mineral surface by influencing  
342 the orientation of near water molecules (Yakobi-Hancock et al., 2013). To sum up, the little or no  
343 effect of carbonate and water-soluble coatings, the unobvious suppression effect of  $H^+$ , and the  
344 enhancement effect of  $NH_4^+/K^+$  and hydrogen bond might act together and finally present the  
345 non-suppression effect observed in this study.

#### 346 **4 Conclusions**

347 To our knowledge, this work is the first to investigate the influence of anthropogenic pollution  
348 on the ice nucleation of airborne mineral dust based on size-resolved Asian dust samples aged in  
349 the real atmosphere. The chemical modification of AAD particles was confirmed by combining  
350 the air quality conditions during sampling periods, physical and chemical properties of collected  
351 particles, and microscopic particle morphology. As the characterization parameters of main  
352 products of heterogeneous reactions, the mass fraction of  $Ca^{2+}$  in element Ca and the mean  
353 relative mass proportions of supermicron  $Ca^{2+}$  increased by 67.0% and 3.5-11.2% in AAD  
354 particles, respectively. Although the AAD particles have been notably aged by anthropogenic  
355 pollution, their total  $N_{INP}$  and total  $n_s(T)$  were consistent with those of AD particles (0.62-1.18  
356 times) without a statistically significant difference. From a size-resolved perspective,  $N_{INP}$  and  
357  $n_s(T)$  of supermicron particles for AAD were nearly equal or even slightly higher compared  
358 with AD samples (0.64-4.34 times at -18 °C). Thus, we conclude that anthropogenic pollution  
359 does not reduce the INP concentrations and INA of Asian dust in the atmosphere.

360 This study advances the scientific understanding about the effects of anthropogenic pollution on  
361 the INA of Asian dust and will contribute to subsequent laboratory studies to further elucidate  
362 the combined effect of multi-species association on dust aging. Furthermore, the significant  
363 implications of this study are more embodied in the regional and global climatic effects. The  
364 dust-driven droplet freezing has been underestimated in model studies (Villanueva et al., 2021).  
365 Following previous understanding assuming that the aging process always significantly impairs  
366 dust freezing, the bias in simulations of cloud microphysical processes and assessments of  
367 radiative effect will further increase under increasing anthropogenic activity scenarios.

368 **Acknowledgments**

369 This work was supported by National Natural Research Foundation of China (NSFC, grant no.  
370 42011530121, 91844301) and Ministry of Science and Technology (MOST, grant no.  
371 2019YFC0214701). We gratefully acknowledge the China Meteorological Administration for the  
372 provision of the forecast and monitoring of Asian dust storm and the China National  
373 Environmental Monitoring Centre for the air quality monitoring data used in this paper.

374 **Conflict of Interest**

375 The authors declare no conflicts of interest relevant to this study.

376 **Data Availability Statement**

377 The data that support the findings of this study are available at this site  
378 (<http://doi.org/10.5281/zenodo.6578828>).

379 **References**

- 380 Atkinson, J. D., B. J. Murray, M. T. Woodhouse, T. F. Whale, K. J. Baustian, K. S. Carslaw, et al. (2013). The  
381 importance of feldspar for ice nucleation by mineral dust in mixed-phase clouds. *Nature*, *498*(7454), 355-358.  
382 doi:10.1038/nature12278
- 383 Augustin-Bauditz, S., H. Wex, S. Kanter, M. Ebert, D. Niedermeier, F. Stolz, et al. (2014). The immersion mode ice  
384 nucleation behavior of mineral dusts: A comparison of different pure and surface modified dusts. *Geophysical*  
385 *Research Letters*, *41*(20), 7375-7382. doi:10.1002/2014gl061317
- 386 Barbieri, M. (2016). The Importance of Enrichment Factor (EF) and Geoaccumulation Index (Igeo) to Evaluate the  
387 Soil Contamination. *Journal of Geology & Geophysics*, *5*(1). doi:10.4172/2381-8719.1000237
- 388 Bi, K., G. R. McMeeking, D. P. Ding, E. J. T. Levin, P. J. DeMott, D. L. Zhao, et al. (2019). Measurements of Ice  
389 Nucleating Particles in Beijing, China. *Journal of Geophysical Research: Atmospheres*, *124*(14), 8065-8075.  
390 doi:10.1029/2019jd030609
- 391 Boose, Y., B. Sierau, M. I. García, S. Rodríguez, A. Alastuey, C. Linke, et al. (2016). Ice nucleating particles in the  
392 Saharan Air Layer. *Atmospheric Chemistry and Physics*, *16*(14), 9067-9087. doi:10.5194/acp-16-9067-2016
- 393 Chen, J., X. Y. Pei, H. Wang, J. C. Chen, Y. S. Zhu, M. J. Tang, & Z. J. Wu. (2018a). Development,  
394 Characterization, and Validation of a Cold Stage-Based Ice Nucleation Array (PKU-INA). *Atmosphere*, *9*(9), 13.  
395 doi:10.3390/atmos9090357
- 396 Chen, J., Z. J. Wu, S. Augustin-Bauditz, S. Grawe, M. Hartmann, X. Y. Pei, et al. (2018b). Ice-nucleating particle  
397 concentrations unaffected by urban air pollution in Beijing, China. *Atmospheric Chemistry and Physics*, *18*(5),  
398 3523-3539. doi:10.5194/acp-18-3523-2018
- 399 Chen, J. C., Z. J. Wu, J. Chen, N. Reicher, X. Fang, Y. Rudich, & M. Hu. (2021). Size-resolved atmospheric ice-  
400 nucleating particles during East Asian dust events. *Atmospheric Chemistry and Physics*, *21*(5), 3491-3506.  
401 doi:10.5194/acp-21-3491-2021
- 402 Connolly, P. J., O. Möhler, P. R. Field, H. Saathoff, R. Burgess, T. Choulaton, & M. Gallagher. (2009). Studies of  
403 heterogeneous freezing by three different desert dust samples. *Atmos. Chem. Phys.*, *9*(8), 2805-2824.  
404 doi:10.5194/acp-9-2805-2009

- 405 Cziczo, D. J., K. D. Froyd, S. J. Gallavardin, O. Moehler, S. Benz, H. Saathoff, & D. M. Murphy. (2009).  
406 Deactivation of ice nuclei due to atmospherically relevant surface coatings. *Environmental Research Letters*, 4(4).  
407 doi:10.1088/1748-9326/4/4/044013
- 408 DeMott, P. J., O. Möhler, D. J. Cziczo, N. Hiranuma, M. D. Petters, S. S. Petters, et al. (2018). The Fifth  
409 International Workshop on Ice Nucleation phase 2 (FIN-02): laboratory intercomparison of ice nucleation  
410 measurements. *Atmospheric Measurement Techniques*, 11(11), 6231-6257. doi:10.5194/amt-11-6231-2018
- 411 Fairlie, T. D., D. J. Jacob, J. E. Dibb, B. Alexander, M. A. Avery, A. van Donkelaar, & L. Zhang. (2010). Impact of  
412 mineral dust on nitrate, sulfate, and ozone in transpacific Asian pollution plumes. *Atmospheric Chemistry and  
413 Physics*, 10(8), 3999-4012. doi:10.5194/acp-10-3999-2010
- 414 Fang, T., H. Guo, L. Zeng, V. Verma, A. Nenes, & R. J. Weber. (2017). Highly Acidic Ambient Particles, Soluble  
415 Metals, and Oxidative Potential: A Link between Sulfate and Aerosol Toxicity. *Environmental Science &  
416 Technology*, 51(5), 2611-2620. doi:10.1021/acs.est.6b06151
- 417 Froyd, K. D., P. Yu, G. P. Schill, C. A. Brock, A. Kupc, C. J. Williamson, et al. (2022). Dominant role of mineral  
418 dust in cirrus cloud formation revealed by global-scale measurements. *Nature Geoscience*. doi:10.1038/s41561-022-  
419 00901-w
- 420 Harrison, A. D., K. Lever, A. Sanchez-Marroquin, M. A. Holden, T. F. Whale, M. D. Tarn, et al. (2019). The ice-  
421 nucleating ability of quartz immersed in water and its atmospheric importance compared to K-feldspar. *Atmospheric  
422 Chemistry and Physics*, 19(17), 11343-11361. doi:10.5194/acp-19-11343-2019
- 423 Harrison, A. D., T. F. Whale, M. A. Carpenter, M. A. Holden, L. Neve, D. O'Sullivan, et al. (2016). Not all feldspars  
424 are equal: a survey of ice nucleating properties across the feldspar group of minerals. *Atmospheric Chemistry and  
425 Physics*, 16(17), 10927-10940. doi:10.5194/acp-16-10927-2016
- 426 Hartmann, M., T. Blunier, S. O. Brügger, J. Schmale, M. Schwikowski, A. Vogel, et al. (2019). Variation of Ice  
427 Nucleating Particles in the European Arctic Over the Last Centuries. *Geophysical Research Letters*, 46(7), 4007-  
428 4016. doi:10.1029/2019GL082311
- 429 He, Y., F. Yi, Y. Yi, F. Liu, & Y. Zhang. (2021). Heterogeneous Nucleation of Midlevel Cloud Layer Influenced by  
430 Transported Asian Dust Over Wuhan (30.5°N, 114.4°E), China. *Journal of Geophysical Research: Atmospheres*,  
431 126(2). doi:10.1029/2020JD033394
- 432 Heim, E. W., J. Dibb, E. Scheuer, P. C. Jost, B. A. Nault, J. L. Jimenez, et al. (2020). Asian dust observed during  
433 KORUS-AQ facilitates the uptake and incorporation of soluble pollutants during transport to South Korea.  
434 *Atmospheric Environment*, 224. doi:10.1016/j.atmosenv.2020.117305
- 435 Hoose, C., & O. Mohler. (2012). Heterogeneous ice nucleation on atmospheric aerosols: a review of results from  
436 laboratory experiments. *Atmospheric Chemistry and Physics*, 12(20), 9817-9854. doi:10.5194/acp-12-9817-2012
- 437 Huang, K., G. Zhuang, J. Li, Q. Wang, Y. Sun, Y. Lin, & J. S. Fu. (2010). Mixing of Asian dust with pollution  
438 aerosol and the transformation of aerosol components during the dust storm over China in spring 2007. *Journal of  
439 Geophysical Research*, 115. doi:10.1029/2009JD013145
- 440 Kanji, Z. A., L. Ladino, H. Wex, Y. Boose, M. Burkert-Kohn, D. Cziczo, & M. Krämer. (2017). Ice Formation and  
441 Evolution in Clouds and Precipitation: Measurement and Modeling Challenges. Chapter 1: Overview of Ice  
442 Nucleating Particles. *Meteorological Monographs*, 58, 1-25. doi:10.1175/AMSMONOGRAPHS-D-0006.1
- 443 Kanji, Z. A., R. C. Sullivan, M. Niemand, P. J. DeMott, A. J. Prenni, C. Chou, et al. (2019). Heterogeneous ice  
444 nucleation properties of natural desert dust particles coated with a surrogate of secondary organic aerosol.  
445 *Atmospheric Chemistry and Physics*, 19(7), 5091-5110. doi:10.5194/acp-19-5091-2019
- 446 Kawai, K., H. Matsui, & Y. Tobo. (2021). High Potential of Asian Dust to Act as Ice Nucleating Particles in Mixed-  
447 Phase Clouds Simulated With a Global Aerosol-Climate Model. *Journal of Geophysical Research: Atmospheres*,  
448 126(12). doi:10.1029/2020jd034263
- 449 Kiselev, A., F. Bachmann, P. Pedevilla, S. J. Cox, A. Michaelides, D. Gerthsen, & T. Leisner. (2017). Active sites in  
450 heterogeneous ice nucleation—the example of K-rich feldspars. *Science*, 355(6323), 367-371.  
451 doi:10.1126/science.aai8034
- 452 Kulkarni, G., K. Zhang, C. Zhao, M. Nandasiri, V. Shutthanandan, X. Liu, et al. (2015). Ice formation on nitric acid-  
453 coated dust particles: Laboratory and modeling studies. *Journal of Geophysical Research: Atmospheres*, 120(15),  
454 7682-7698. doi:10.1002/2014jd022637
- 455 Kumar, A., C. Marcolli, B. Luo, & T. Peter. (2018). Ice nucleation activity of silicates and aluminosilicates in pure  
456 water and aqueous solutions – Part 1: The K-feldspar microcline. *Atmospheric Chemistry and Physics*, 18(10), 7057-  
457 7079. doi:10.5194/acp-18-7057-2018
- 458 Laskin, A., M. Iedema, A. Ichkovich, E. Graber, I. Taraniuk, & Y. Rudich. (2005). Direct observation of completed  
459 processed calcium carbonate dust particles. *Faraday Discussions*, 130, 453-468; discussion 491.  
460 doi:10.1039/B417366J

- 461 Lawson, D. R., & J. W. Winchester. (1979). Standard Crustal Aerosol as a Reference for Elemental Enrichment  
462 Factors. *Atmospheric Environment*, 13(7), 925-930. doi:10.1016/0004-6981(79)90003-9
- 463 Li, W. J., & L. Y. Shao. (2009). Observation of nitrate coatings on atmospheric mineral dust particles. *Atmos. Chem.*  
464 *Phys.*, 9(6), 1863-1871. doi:10.5194/acp-9-1863-2009
- 465 Li, W. J., L. Y. Shao, Z. B. Shi, J. M. Chen, L. X. Yang, Q. Yuan, et al. (2014). Mixing state and hygroscopicity of  
466 dust and haze particles before leaving Asian continent. *Journal of Geophysical Research-Atmospheres*, 119(2),  
467 1044-1059. doi:10.1002/2013jd021003
- 468 Li, W. J., L. Y. Shao, D. Z. Zhang, C. U. Ro, M. Hu, X. H. Bi, et al. (2016). A review of single aerosol particle  
469 studies in the atmosphere of East Asia: morphology, mixing state, source, and heterogeneous reactions. *Journal of*  
470 *Cleaner Production*, 112, 1330-1349. doi:10.1016/j.jclepro.2015.04.050
- 471 Lohmann, U., F. Lüönd, & F. Mahrt. (2016). *An Introduction to Clouds: From the Microscale to Climate*.  
472 Cambridge: Cambridge University Press.
- 473 Losey, D. J., S. K. Sihvonen, D. P. Veghte, E. Chong, & M. A. Freedman. (2018). Acidic processing of fly ash:  
474 chemical characterization, morphology, and immersion freezing. *Environmental Science: Processes & Impacts*,  
475 20(11), 1581-1592. doi:10.1039/C8EM00319J
- 476 Marple, V. A., K. L. Rubow, & S. M. Behm. (1991). A Microorifice Uniform Deposit Impactor (MOUDI):  
477 Description, Calibration, and Use. *Aerosol Science and Technology*, 14(4), 434-446.  
478 doi:10.1080/02786829108959504
- 479 McNaughton, C. S., A. D. Clarke, V. Kapustin, Y. Shinozuka, S. G. Howell, B. E. Anderson, et al. (2009).  
480 Observations of heterogeneous reactions between Asian pollution and mineral dust over the Eastern North Pacific  
481 during INTEX-B. *Atmos. Chem. Phys.*, 9(21), 8283-8308. doi:10.5194/acp-9-8283-2009
- 482 Meng, Z., L. Wu, X. Xu, W. Xu, R. Zhang, X. Jia, et al. (2020). Changes in ammonia and its effects on PM<sub>2.5</sub>  
483 chemical property in three winter seasons in Beijing, China. *Sci Total Environ*, 749, 142208.  
484 doi:10.1016/j.scitotenv.2020.142208
- 485 Murray, B. J., D. O'Sullivan, J. D. Atkinson, & M. E. Webb. (2012). Ice nucleation by particles immersed in  
486 supercooled cloud droplets. *Chem Soc Rev*, 41(19), 6519-6554. doi:10.1039/c2cs35200a
- 487 Niedermeier, D., S. Augustin-Bauditz, S. Hartmann, H. Wex, K. Ignatius, & F. Stratmann. (2015). Can we define an  
488 asymptotic value for the ice active surface site density for heterogeneous ice nucleation? *Journal of Geophysical*  
489 *Research: Atmospheres*, 120(10), 5036-5046. doi:10.1002/2014jd022814
- 490 Niedermeier, D., S. Hartmann, R. A. Shaw, D. Covert, T. F. Mentel, J. Schneider, et al. (2010). Heterogeneous  
491 freezing of droplets with immersed mineral dust particles – measurements and parameterization. *Atmos. Chem.*  
492 *Phys.*, 10(8), 3601-3614. doi:10.5194/acp-10-3601-2010
- 493 Niemand, M., O. Möhler, B. Vogel, H. Vogel, C. Hoose, P. Connolly, et al. (2012). A Particle-Surface-Area-Based  
494 Parameterization of Immersion Freezing on Desert Dust Particles. *Journal of the Atmospheric Sciences*, 69(10),  
495 3077-3092. doi:10.1175/jas-d-11-0249.1
- 496 O'Sullivan, D., B. J. Murray, T. L. Malkin, T. F. Whale, N. S. Umo, J. D. Atkinson, et al. (2014). Ice nucleation by  
497 fertile soil dusts: relative importance of mineral and biogenic components. *Atmos. Chem. Phys.*, 14(4), 1853-1867.  
498 doi:10.5194/acp-14-1853-2014
- 499 Peckhaus, A., A. Kiselev, T. Hiron, M. Ebert, & T. Leisner. (2016). A comparative study of K-rich and Na/Ca-rich  
500 feldspar ice-nucleating particles in a nanoliter droplet freezing assay. *Atmospheric Chemistry and Physics*, 16(18),  
501 11477-11496. doi:10.5194/acp-16-11477-2016
- 502 Pratt, K. A., P. J. DeMott, J. R. French, Z. Wang, D. L. Westphal, A. J. Heymsfield, et al. (2009). In situ detection of  
503 biological particles in cloud ice-crystals. *Nature Geoscience*, 2(6), 398-401. doi:10.1038/ngeo521
- 504 Pye, H. O. T., A. Nenes, B. Alexander, A. P. Ault, M. C. Barth, S. L. Clegg, et al. (2020). The acidity of  
505 atmospheric particles and clouds. *Atmos. Chem. Phys.*, 20(8), 4809-4888. doi:10.5194/acp-20-4809-2020
- 506 Reicher, N., L. Segev, & Y. Rudich. (2018). The WeIzmann Supercooled Droplets Observation on a Microarray  
507 (WISDOM) and application for ambient dust. *Atmospheric Measurement Techniques*, 11(1), 233-248.  
508 doi:10.5194/amt-11-233-2018
- 509 Schill, G. P., P. J. DeMott, E. W. Emerson, A. M. C. Rauker, J. K. Kodros, K. J. Suski, et al. (2020). The  
510 contribution of black carbon to global ice nucleating particle concentrations relevant to mixed-phase clouds.  
511 *Proceedings of the National Academy of Sciences*, 117(37), 22705. doi:10.1073/pnas.2001674117
- 512 Song, S., A. Nenes, M. Gao, Y. Zhang, P. Liu, J. Shao, et al. (2019). Thermodynamic Modeling Suggests Declines  
513 in Water Uptake and Acidity of Inorganic Aerosols in Beijing Winter Haze Events during 2014/2015–2018/2019.  
514 *Environmental Science & Technology Letters*, 6(12), 752-760. doi:10.1021/acs.estlett.9b00621

- 515 Sullivan, R. C., L. Miñambres, P. J. DeMott, A. J. Prenni, C. M. Carrico, E. J. T. Levin, & S. M. Kreidenweis.  
516 (2010a). Chemical processing does not always impair heterogeneous ice nucleation of mineral dust particles.  
517 *Geophysical Research Letters*, 37(24), n/a-n/a. doi:10.1029/2010gl045540
- 518 Sullivan, R. C., M. D. Petters, P. J. DeMott, S. M. Kreidenweis, H. Wex, D. Niedermeier, et al. (2010b). Irreversible  
519 loss of ice nucleation active sites in mineral dust particles caused by sulphuric acid condensation. *Atmos. Chem.*  
520 *Phys.*, 10(23), 11471-11487. doi:10.5194/acp-10-11471-2010
- 521 Textor, C., M. Schulz, S. Guibert, S. Kinne, Y. Balkanski, S. Bauer, et al. (2006). Analysis and quantification of the  
522 diversities of aerosol life cycles within AeroCom. *Atmos. Chem. Phys.*, 6(7), 1777-1813. doi:10.5194/acp-6-1777-  
523 2006
- 524 Tobo, Y., P. J. DeMott, M. Raddatz, D. Niedermeier, S. Hartmann, S. M. Kreidenweis, et al. (2012). Impacts of  
525 chemical reactivity on ice nucleation of kaolinite particles: A case study of levoglucosan and sulfuric acid.  
526 *Geophysical Research Letters*, 39(19), n/a-n/a. doi:10.1029/2012gl053007
- 527 Underwood, G. M., C. H. Song, M. Phadnis, G. R. Carmichael, & V. H. Grassian. (2001). Heterogeneous reactions  
528 of NO<sub>2</sub> and HNO<sub>3</sub> on oxides and mineral dust: A combined laboratory and modeling study. *Journal of Geophysical*  
529 *Research: Atmospheres*, 106(D16), 18055-18066. doi:10.1029/2000JD900552
- 530 Uno, I., K. Eguchi, K. Yumimoto, T. Takemura, A. Shimizu, M. Uematsu, et al. (2009). Asian dust transported one  
531 full circuit around the globe. *Nature Geoscience*, 2(8), 557-560. doi:10.1038/ngeo583
- 532 Vali, G. (1971). Quantitative evaluation of experimental results on the heterogeneous freezing nucleation of  
533 supercooled liquids. *Journal of the Atmospheric Sciences*, 28(3), 402-409.
- 534 Vali, G., P. J. DeMott, O. Möhler, & T. F. Whale. (2015). Technical Note: A proposal for ice nucleation  
535 terminology. *Atmos. Chem. Phys.*, 15(18), 10263-10270. doi:10.5194/acp-15-10263-2015
- 536 Villanueva, D., D. Neubauer, B. Gasparini, L. Ickes, & I. Tegen. (2021). Constraining the Impact of Dust-Driven  
537 Droplet Freezing on Climate Using Cloud-Top-Phase Observations. *Geophysical Research Letters*, 48(11).  
538 doi:10.1029/2021gl092687
- 539 Wei, F., C. Zheng, J. Chen, & Y. Wu. (1991). Study on the Background Contents on 61 Elements of Soils in China.  
540 *Environmental Science*, 12(4), 12-19. doi:10.13227/j.hjx.1991.04.005
- 541 Wex, H., P. J. DeMott, Y. Tobo, S. Hartmann, M. Rösch, T. Clauss, et al. (2014). Kaolinite particles as ice nuclei:  
542 learning from the use of different kaolinite samples and different coatings. *Atmos. Chem. Phys.*, 14(11), 5529-5546.  
543 doi:10.5194/acp-14-5529-2014
- 544 Whale, T. F., M. A. Holden, T. W. Wilson, D. O'Sullivan, & B. J. Murray. (2018). The enhancement and  
545 suppression of immersion mode heterogeneous ice-nucleation by solutes. *Chem Sci*, 9(17), 4142-4151.  
546 doi:10.1039/c7sc05421a
- 547 Whale, T. F., B. J. Murray, amp, apos, D. Sullivan, T. W. Wilson, et al. (2015). A technique for quantifying  
548 heterogeneous ice nucleation in microlitre supercooled water droplets. *Atmospheric Measurement Techniques*, 8(6),  
549 2437-2447. doi:10.5194/amt-8-2437-2015
- 550 Worthy, S. E., A. Kumar, Y. Xi, J. Yun, J. Chen, C. Xu, et al. (2021). The effect of (NH<sub>4</sub>)<sub>2</sub>SO<sub>4</sub> on the freezing  
551 properties of non-mineral dust ice-nucleating substances of atmospheric relevance. *Atmos. Chem. Phys.*, 21(19),  
552 14631-14648. doi:10.5194/acp-21-14631-2021
- 553 Wu, C., S. Zhang, G. Wang, S. Lv, D. Li, L. Liu, et al. (2020). Efficient Heterogeneous Formation of Ammonium  
554 Nitrate on the Saline Mineral Particle Surface in the Atmosphere of East Asia during Dust Storm Periods. *Environ*  
555 *Sci Technol*, 54(24), 15622-15630. doi:10.1021/acs.est.0c04544
- 556 Xie, Y., G. Wang, X. Wang, J. Chen, Y. Chen, G. Tang, et al. (2020). Nitrate-dominated PM<sub>2.5</sub> and elevation of  
557 particle pH observed in urban Beijing during the winter of 2017. *Atmospheric Chemistry and Physics*, 20(8), 5019-  
558 5033. doi:10.5194/acp-20-5019-2020
- 559 Yakobi-Hancock, J. D., L. A. Ladino, & J. P. D. Abbatt. (2013). Feldspar minerals as efficient deposition ice nuclei.  
560 *Atmospheric Chemistry and Physics*, 13(22), 11175-11185. doi:10.5194/acp-13-11175-2013
- 561 Yun, J., A. Kumar, N. Removski, A. Shchukarev, N. Link, J.-F. Boily, & A. K. Bertram. (2021). Effects of  
562 Inorganic Acids and Organic Solutes on the Ice Nucleating Ability and Surface Properties of Potassium-Rich  
563 Feldspar. *Acs Earth and Space Chemistry*, 5(5), 1212-1222. doi:10.1021/acsearthspacechem.1c00034
- 564 Yun, J., N. Link, A. Kumar, A. Shchukarev, J. Davidson, A. Lam, et al. (2020). Surface Composition Dependence  
565 on the Ice Nucleating Ability of Potassium-Rich Feldspar. *Acs Earth and Space Chemistry*, 4(6), 873-881.  
566 doi:10.1021/acsearthspacechem.0c00077
- 567 Zhao, B., Y. Wang, Y. Gu, K.-N. Liou, J. H. Jiang, J. Fan, et al. (2019). Ice nucleation by aerosols from  
568 anthropogenic pollution. *Nature Geoscience*, 12(8), 602-607. doi:10.1038/s41561-019-0389-4

- 569 Zhao, M., S. Wang, J. Tan, Y. Hua, D. Wu, & J. Hao. (2016). Variation of Urban Atmospheric Ammonia Pollution  
570 and its Relation with PM<sub>2.5</sub> Chemical Property in Winter of Beijing, China. *Aerosol and Air Quality Research*,  
571 16(6), 1390-1402. doi:10.4209/aaqr.2015.12.0699
- 572 Zhu, J. L., & J. E. Penner. (2020). Radiative forcing of anthropogenic aerosols on cirrus clouds using a hybrid ice  
573 nucleation scheme. *Atmospheric Chemistry and Physics*, 20(13), 7801-7827. doi:10.5194/acp-20-7801-2020
- 574 Zhu, T., J. Shang, & D. F. Zhao. (2011). The roles of heterogeneous chemical processes in the formation of an air  
575 pollution complex and gray haze. *Science China-Chemistry*, 54(1), 145-153. doi:10.1007/s11426-010-4181-y
- 576 Zolles, T., J. Burkart, T. Hausler, B. Pummer, R. Hitzemberger, & H. Grothe. (2015). Identification of ice nucleation  
577 active sites on feldspar dust particles. *J Phys Chem A*, 119(11), 2692-2700. doi:10.1021/jp509839x
- 578